Chemosphere 311 (2023) 137086

Contents lists available at ScienceDirect

Chemosphere

journal homepage: www.elsevier.com/locate/chemosphere

Evaluation of antimony availability in a mining context: Impact for the environment, and for mineral exploration and exploitation.

José María Esbrí [a,b,*], Carmelo M. Minang [a], Sofía Rivera [a], Mercedes Madrid-Illescas [a,c], Eva García-Noguero [a], Ana González-Valoys [a,d], Maite Maguregui [e], Hugues Thouin [f], Fabienne Battaglia-Brunet [f], Eric Gloaguen [f], Pablo León Higueras [a]

[a] Instituto de Geología Aplicada, Escuela de Ingeniería Minera e Industrial de Almadén, Universidad de Castilla-La Mancha, Plaza M. Meca 1, Almadén, Ciudad Real 13400, Spain
[b] Departamento de Mineralogía y Petrología, Universidad Complutense de Madrid, José Antonio Novais 12, 28040 Madrid, Spain
[c] Departamento de Ingeniería Química, Universidad de Castilla-La Mancha, E.I.M.I. 13400 Almadén, Ciudad Real, Spain
[d] Centro Experimental de Ingeniería, Universidad Tecnológica de Panamá, Vía Tocumen, 0819-07289 Panama City, Panama
[e] Departamento de Química Analítica, Universidad del País Vasco, Facultad de Farmacia, P.° de la Universidad, 7, 01006 Vitoria-Gasteiz, Álava, Spain
[f] ISTO, UMR7327, Université d'Orléans, CNRS, BRGM, F-45071 Orléans, France

HIGHLIGHTS

- More than 99% Sb was in the residual fraction in BCR fractionation applied to soil.
- Soil health can be affected due to poor dehydrogenase activities in the studied soil.
- Pollutants from soil to Quercus leaves were few, with bioaccumulation factors <0.1520
- Low Sb (III) formation and toxicological risk.

GRAPHICAL ABSTRACT

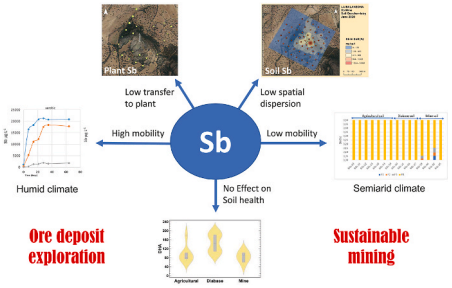

ARTICLE INFO

Keywords:
Sb
Quercus
Availability
Stibnite
Enzymatic activity
BCR

ABSTRACT

This work aims to establish Sb mobility, its transfer to biota and its effect on soil health in a semi-arid climate. The results show the presence of stibnite (Sb_2S_3) as the main primary Sb compound, bindhemite ($Pb_2Sb_2O_6(O,OH)$), and minor proportions of stibiconite ($(Sb^{3+}(Sb^{5+})_2O_6(OH)$) as oxidised Sb species. This research also observes very high total Sb contents in mining materials (max: 20,000 mg kg^{-1}) and soils (400–3000 mg kg^{-1}), with physical dispersion around mining materials restricted to 450 m. The soil-to-plant transfer is very low, (bioaccumulation factor: 0.0002–0.1520). Most Sb remains in a residual fraction (99.9%), a very low fraction is bound to Fe and Mn oxy-hydroxides or organic matter, and a negligible proportion of Sb is leachable. The higher Sb mobility rates has been found under oxidising conditions with a long contact time between solids and water. The main factors that explain the poor Sb mobility and dispersion in the mining area are the low annual rainfall rates that slow down the Sb mobilisation process and the scarce formation of oxidised Sb compounds. All these data suggest poor Sb (III) formation and a low toxicological risk in the area associated with past mining activities.

* Departamento de Mineralogía y Petrología, Universidad Complutense de Madrid, José Antonio Novais 12, 28040 Madrid, Spain.
E-mail address: jesbri@ucm.es (J.M. Esbrí).

https://doi.org/10.1016/j.chemosphere.2022.137086
Received 14 July 2022; Received in revised form 28 October 2022; Accepted 30 October 2022
Available online 2 November 2022

The low mobility of Sb suggests advantages for future sustainable mining of such ore deposits in a semi-arid climate and is also indicative of the limitations of geochemical exploration in the search for new Sb deposits.

1. Introduction and background

Antimony (Sb) has been considered by the European Union (EU) to be a Critical Raw Material, given the relevance of this element for European economy and its poor availability. China (74%), Tajikistan (8%) and Russia (4%) are the main countries that supply Sb worldwide (European Union, 2020). In 2020, the EU totally depended on imports to ensure the supply of this element, which is essential in industrial sectors like flame retardants, defence applications and lead-acid batteries (European Commission, 2020). The EU has been promoting research to solve this problem by reusing and recovering Sb in mining or industrial facilities, and by also promoting the identification of Sb ore deposits to be sustainably exploited. Within the EU Cofunded ERA-MIN Joint Call 2021 framework (ERAMIN, 2021), the AUREOLE research project aims to generate the best prospecting and exploitation techniques for Sb deposits to increase the potential Sb resources in western Europe (France, Spain and Portugal). This last aspect is particularly significant in the circular economy context adopted by the EU, where the value of products, materials and resources will be maintained in economy as long as possible by minimising waste generation. Although Sb has a high recycling input rate, developing the circular economy concept will be essential to ensure its production.

The Iberian Peninsula encompasses all the Sb deposit types, where the main mineral carrier of Sb is stibnite (Sb_2S_3), and these antimony-bearing deposits represent the largest Sb deposits worldwide. Other scarce types of deposits where Sb is a co- or by-product are represented by intrusion-related gold and polymetallic deposits, where Sb is hosted by sulfosalts (Schwartz-Schampera et al., 2014). This study focuses on stibnite deposits. According to Gumiel and Arribas (1987), there are 61 Sb deposits and occurrences, including vein-type deposits, strata-bound deposits and Sb deposits in volcanic dykes, in the Iberian Peninsula. Most of these Sb deposits are related to the Variscan orogeny and preferentially located in the southern Central Iberian zone. The most frequent mineral association is quartz-stibnite (La Balanzona, among others), but there are others with important deposits like quartz-stibnite-gold (Mari-Rosa mine, Ortega et al., 1996), carbonate-quartz-stibnite-sphalerite-gold (Ribeiro da Igreja mine), carbonate-quartz-stibnite-galena-silver (Diogenes mine), quartz-stibnite-sphalerite (Nazarena mine, Boixereu Vila and Fernández-Leyva, 2019), quartz-stibnite-scheelite (San Antonio mine, Arribas and Gumiel, 1984; Álvarez-Ayuso et al., 2022) and quartz-stibnite-covellite (Accesos mine, characteristic of the southern branch of the Variscan belt) (Gumiel and Arribas, 1987). Accordingly, the diversity of mineral associations is wide in the Iberian Peninsula, which implies considerable complexity when evaluating Sb mobility in such heterogeneous contexts. Pyrite, chalcopyrite and arsenopyrite are common in some of these deposits and present an acid mine drainage (AMD) generation potential that would increase the mobility of not only Sb, but of other metals and metalloids (Bolan et al., 2022). However, other factors may be involved in Sb mobility, especially climate conditions, which determine the weathering rate of these mineral deposits (Casiot et al., 2007; Borčinová Radkova et al., 2020).

In ore deposits, Sb can be released by stibnite dissolution under oxidising conditions, which produces several Sb secondary minerals like tripuhyite ($FeSbO_4$), senarmontite (Sb_2O_3), romeite ($Ca_2Sb_2O_6OH$), cervantite (Sb_2O_4), kermesite (Sb_2S_2O) and valentinite (Sb_2O_3) (Courtin-Nomade et al., 2012; Roper et al., 2012). Sb mobility is related to the four oxidation Sb states in the environment (−III, 0, III, V), and Sb (III) and Sb (V) are components of the most frequent mineral species. In initial stibnite weathering stages, Sb (III) usually forms valentinite ($Sb_2^{III}O_3$), and a mixture of Sb (III) and Sb (V) forms stibiconite ($Sb^{III}(Sb^{V})_2O_6(OH)$) (Szakall et al., 2000; Ashley et al., 2003). Sb (III) is generally expected to be the major phase under anoxic conditions, with Sb (V) under aerobic conditions (Filella et al., 2007). If Sb (III) is detected in groundwater, Sb (V) is generally the main aqueous Sb species in surface waters (Li et al., 2016). The important factors involved in Sb mobility are pH and microorganisms (Loni et al., 2020). Sb in soil is preferentially absorbed in Fe oxyhydroxides (Johnston et al., 2020). The role of SOM in Sb retention is still being discussed because bioavailable Sb retention processes have been described for plants (Steely et al., 2007), as have dissolution processes after applying compost to contaminated soils (Verbeeck et al., 2020).

Murciego et al. (2007) described Sb accumulation patterns for three shrub plant species: *Cytisus striatus*, *Cistus ladanifer* and *Dittrichia viscosa*. Low Sb concentrations were found in *Cytisus striatus* (0.06 mg kg^{-1} in the Mari Rosa mine), with higher contents in *Cistus ladanifer* (reaching 79.3 mg kg^{-1} in the San Antonio mine) and much higher ones in *Dittrichia viscosa* (1136 mg kg^{-1} in the San Antonio mine). *Cytisus striatus* presented Sb excluder characteristics, whereas *Dittrichia viscosa* specimens showed significant Sb bioaccumulation.

The present work aims to investigate Sb mobility under outcrop conditions or in abandoned mining exploitations to explore the influence of soil and/or sediment geochemistry on the discovery of Sb deposits, and to predict Sb leachability in reservoirs and mining waste. These two secondary objectives will also contribute to improve methods for prospecting and exploiting this type of deposits. To meet these objectives, an ore deposit type was selected in the Central Iberian area, namely the derelict La Balanzona mine (Córdoba, Spain).

2. Experimental section

2.1. Sampling

The sampling strategy included a first stage to recognise the main Sb mines in the Guadalmez syncline. It was followed by a second phase that consisted in the systematic sampling of the soils and local vegetation in the La Balanzona mine. In the first sampling phase, rock samples, mining waste materials, soils and sediments were collected at the abandoned La Balanzona mining site and also in nearby outcrops (distance <5 km), found following tectonic alignments. Rock samples were collected from outcrops (mainly quartzites) using a geologist's hammer and were bagged with an identifying code. Mining waste materials were collected from dumps using a plastic shovel for finer materials and large ore blocks were collected by hand. Finally, the soil and sediment samples were collected using an Ejkelkamp sampler capable of collecting two samples at different depths: superficial (depth 0–15 cm) and deep (depth 15–30 cm). At each sampling location, three subsamples were collected within a 5-m radius and a composite sample weighing about 4 kg was obtained after mixing.

In the second surveying phase, a sampling network was designed to collect soil samples at the La Balanzona mine. Samples were separated by 120 m, and densification in the mining operations area included a 60-m separation. Fifty-seven soil samples were taken at two depths following the methodology set out in the previous paragraph (Fig. 1).

Samples of *Quercus rotundifolia* leaves (the most ubiquitous and representative vascular plant) were collected from several adult specimens (fully developed trees) in an attempt to sample all the space directions from each tree at an approximate height of 2 m. Each leaf sample was cut from the tree using pruning shears and was stored in a paper envelope labelled with the sample code to be transported to the laboratory.

2.2. Sample preparation

Soil sample preparation included drying at room temperature for 15 days, disaggregation, and homogenisation prior to sieving at 2 mm to obtain two representative aliquots of 50 g: one for the analysis, which was ground in an agate mortar for 2 min until an approximate grain size of 100 μm was obtained; another for the physico-chemical determinations, including reactivity (pH), salt contents (electric conductivity), soil organic carbon (SOC) and dehydrogenase activity (DHA), which remained with their original granulometry. Tree leaves were thoroughly washed with deionised water and dried in an oven at 42 °C for 168 h. Subsequently, leaves were separated from stems by hand using nitrile gloves and ground in a scientific mill.

2.3. Mineralogical characterisation and geochemical analysis

Mineralogical characterisation was conducted using X-Ray Diffraction (XRD) conducted on the milled samples. Diffractograms were obtained at IRICA-UCLM with Bruker D8 Advance A25 equipment during a 15-min work programme. Measured patterns were qualitatively and quantitatively analysed with the Match v.3 and the Fullprof software for Rietveld analyses, respectively (Moore and Reynolds, 1997). Diffractogram interpretation focused on identifying the presence of quartz, Fe oxides and mineral phases containing Sb.

Major and trace elements from the soil and biota samples were quantitatively determined by Energy dispersive X-ray fluorescence (EDXRF) using a Panalytical device (Epsilon 2 model). Each sample was analysed in duplicate during a 24-min run to perform four energy passes for the selected groups of elements. The quality control consisted in analysing both duplicates and certified reference materials: NIST 2710a for soils and BCR62 for leaves.

Total Hg was determined by atomic absorption spectrometry (AAS) with a Lumex RA-915 M device equipped with a Pyro-915+ pyrolysis unit. Samples were pyrolysed at 900 °C according to a gaseous Hg atomisation method, which is drawn by a stream of carrier air at 3 L min^{-1} to the analytical cell (Esbrí et al., 2021). The quality control included the analysis of the previously mentioned certified reference material for the soil and leaf samples, with a recovery rate of 99–105% and 92–114%, respectively.

2.4. Sb mobility and enzymatic activity

Dehydrogenase activity was measured following colorimetric techniques using a Biochrom Libra S60 spectrophotometer (Biochrom, UK) running at 485 nm and according to the triphenyltetrazolium chloride (TTC) method described by Casida (1977), as modified by Barajas (2008) and Montejo et al. (2012). A homogenised soil sample (1.5 g) was placed inside a test tube and mixed with 1.5 mL of deionised water, 0.015 g of $CaCO_3$ and 0.250 mL of TTC (3% v/w) to be vortexed (2 min) and incubated (Memmert In 30) at 37 °C for 24 h. Afterwards, samples were vortexed using methanol as an extractant agent and tubes were centrifuged (Ortoalresa, Unicen 21) at 4000 rpm for 10 min. The

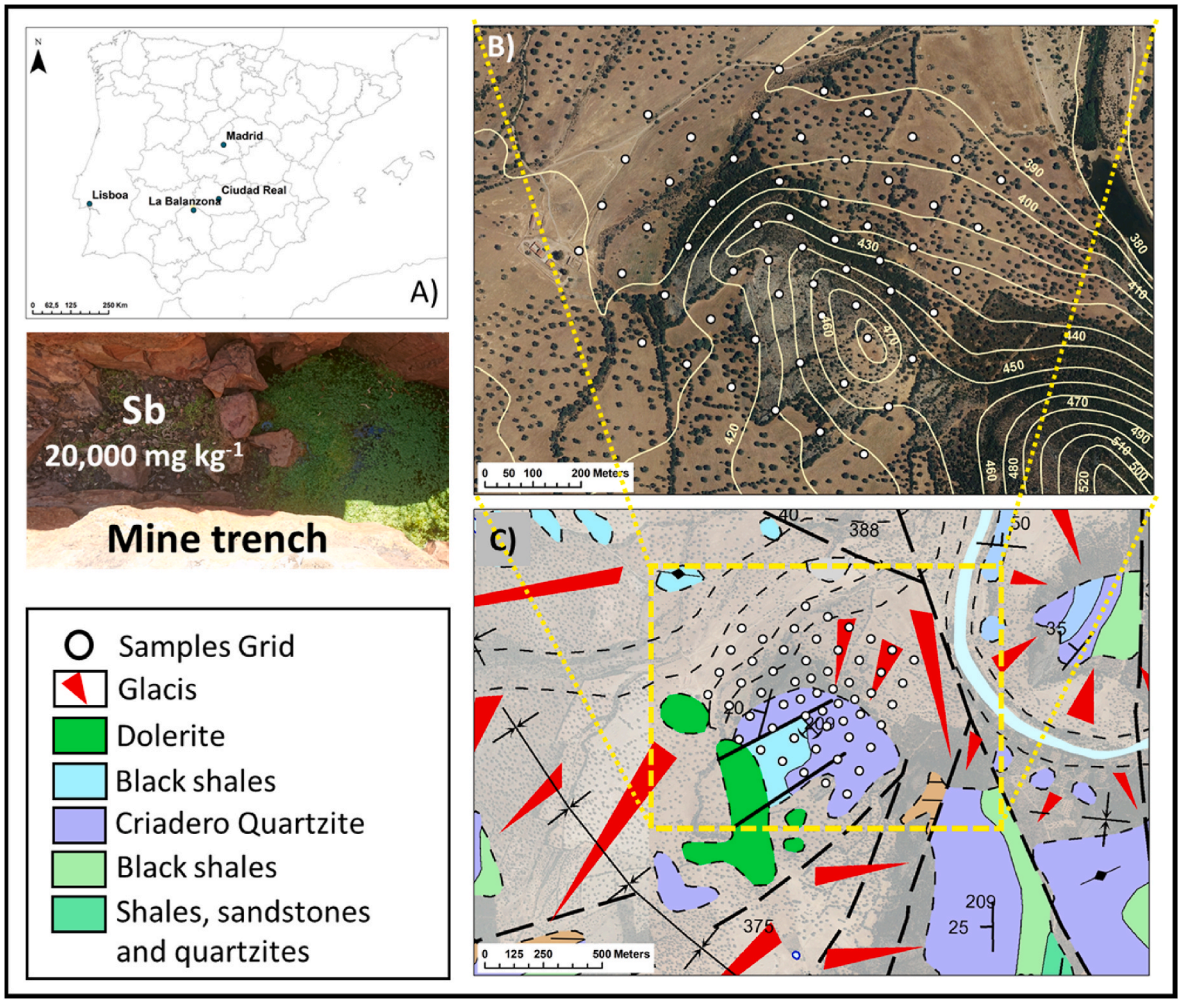

Fig. 1. Sampling grid in the La Balanzona mine. A) Mine site location; B) Orthophotography of the mine site with elevation lines (10 m spacing); C) Geological sketch map.

supernatant was analysed in a UV–visible spectrophotometer at 485 nm (Gonzalez-Valoys et al., 2021). Data were expressed as μg TPF g_{soil}^{-1} day^{-1}.

To study Sb leachability and bioavailability, modified BCR sequential extraction was carried out. This sequential extraction procedure (SEP) consisted in three successive extractions from which three extracts and the residual fraction were obtained. The methodology was based on the BCR method (Quevauviller et al., 1997), adapted to a 4-step scheme as reported by, for instance, Sahuquillo et al. (1999) and Delgado et al. (2011). Briefly, the different SEP steps allowed four fractions to be differentiated: the first fraction (F1), extracted by a solution of 0.11 M acetic acid, releases the species that are soluble in water, easily leached by weak acids and associated with soluble carbonates; the second fraction (F2), extracted by 0.5 M hydroxylamine hydrochloride (pH 1.5 with 2 M nitric acid), consists of easily reducible species associated with Fe and Mn oxy-hydroxides; the third fraction (F3) includes digestion by 8.8 M hydrogen peroxide (several hours at 85 °C) and a later extraction with 1.0 M ammonium acetate (pH 2.0 with concentrated acid nitric), and comprises easily oxidisable species, mainly associated with organic matter and sulphide minerals. The residual fraction was determined by making a calculation between the difference of pseudo-totals and mobile fractions. BCR 701 certified reference material was used to evaluate Pb recovery (between 95 and 98%). As Sb is not certificated in this reference material, its recovery could not be evaluated.

Samples were also subjected to microwave-assisted acid digestion with aqua regia according to EPA method 3051A (USEPA, 2007) to analyse acid-extractable fraction concentrations (Melaku et al., 2005; Higueras et al., 2017). After filtering with Whatman filters (8 μm), the analysis of the total Sb and Pb fractions was performed by High-Resolution Atomic Absorption Spectrometry with Analytic Jenna ContrAA-800D equipment. To quantify Sb, Atomic Fluorescence Spectroscopy by Hydride Generation (AFS-HG) was applied using a PSAnalytical, Millennium Excalibur model with 0.1μ L^{-1} sensitivity for the explored concentration range. Certified reference material NIST 2710A was also digested and analysed in triplicate, with 92% and 95% recovery for Pb and Sb, respectively.

Long-term (2 months) leaching experiments were performed with three soil samples. They presented: high (BA 001; 20,260 mg kg^{-1}), medium (BA 002; 17,352 mg kg^{-1}) and low (BA 003; 3377 mg kg^{-1}) Sb concentrations. Slurries were prepared with 20 g of dry soil and 200 mL of mineral water (composition close to rainwater, Mont Roucous water, pH = 6.38, electrical conductivity = 160 μS cm^{-1}, Cl- = 56 μM, NO_3^- = 24 μM, SO_4^{2-} = 16 μM, Na^+ = 109 μM, K^+ = 7.7 μM, Ca^{2+} = 25 μM, Mg^{2+} = 21 μM). Aerobic incubations were performed in 500 mL erlenmeyer flasks sealed with cotton stoppers. Anaerobic incubations were carried out in 500 mL Shott bottles sealed with rubber stoppers and filled with N_2 85% H_2 15% as a gas phase (1 atm above ambient pressure). Sampling events were run once weekly for the first month, and then at the end of incubation (day 64). After pH measurements, 5 mL samples were filtrated (0.45 μm), acidified with concentrated HNO_3 and then analysed by oven SAA (Varian) for the total Sb determinations.

3. Results and discussion

3.1. Rock and soil samples characterisation

Main mineral phases of the area has been identified on rock samples (quartzite) by XRD as stibnite (Sb_2S_3), with bindehimite ($Pb_2Sb_2O_6(O,OH)$) and stibiconite ($(Sb^{3+}(Sb^{5+})_2O_6(OH)$) as the main oxidised phases.

The results of the multielemental analysis performed with the soil samples showed that Si, Al, Fe, Ti, K, P and Ca were the major elements in decreasing order of concentration, together with Mn, Zr, Sb, Co, Pb, Ba, V, Cr, Zn, Ni, Rb, Sn and Sr as the trace elements in decreasing order of concentration (above 50 mg kg^{-1}). Cu, Y, Yb, As, Nb, Ga, Cs, Mo, Th, Br, Pd and Re were quantified below 50 mg kg^{-1} (Table S1). Quercus leaves showed a more reduced distribution of major elements (Mn > Cl > Eu > Zn > Sn) than soils, with the following most important trace elements in decreasing order of concentration: Ni > Br > Sr > Ce > Rb > Sb > Zr > Pb (Table S1).

With an average SiO_2 content close to 50%, the La Balanzona area soils can be defined as siliceous, with high Fe_2O_3 contents and Sb and Pb as the most important trace elements. These two elements appeared in the area at higher concentrations, while the distribution of the data in a probability plot (Fig. S1) showed that Sb had a background population at very low concentrations, another transition population between 23.4 mg kg^{-1} and 524.8 mg kg^{-1}, and a last anomalous population above 524.8 mg kg^{-1}. This distribution is consistent with the sampling design being so close to the mineralisation and mining area, and with only a few background values among the analysed data. The other trace element obtained at appreciable concentrations was Pb, which showed a different distribution in two populations: one with a broader background (below 380.2 mg kg^{-1}) and another anomalous one above 380.2 mg kg^{-1}. These differences between data populations imply that, although these two elements appeared in the area, there had to be an additional source of anomalous Pb values there to explain these differences, or the Sb and Pb primary mineralisations were not syngenetic. The spatial distribution of these two elements also presented different distribution patterns (Fig. 2).

The average pH value of soils was 6.0 with values close to neutrality. EC values were around 38 μS cm^{-1}, which implies quite low salt content values. SOC contents were 4% on average, which are low, but not particularly rare values for poor developing soils of scarce agricultural use. None of these values showed significant differences between the superficial and deep samples (Table S2) which, according to these variables, implies low degrees of the modification of soil characteristics by mining activity.

3.2. Total and available Sb and Pb concentrations and their spatial distribution

The total Sb concentration in the mining area was around 62-fold higher than the lowest concentration obtained in the agricultural soils located far from the mine (1175.2 mg kg^{-1} vs. 19.4 mg kg^{-1}). The reference Sb value for the Castilla-La Mancha (Spain) soils was 2.76 mg kg^{-1} (Jiménez Ballesta et al., 2010), which was below the minimum total Sb value in the studied samples. Therefore, the entire area could be considered to be Sb-enriched, since the low Sb content reach 7 times this background value. Locally, the reference value must be higher in the Palaeozoic materials of the Guadalmez syncline than in the reference values of the entire Castilla-La Mancha region. The most recent data indicates a total Sb value of 9.1 mg kg^{-1} in syncline soils (Rivera-Jurado et al., 2021), which was around 2-fold lower compared to the minimum concentration recorded at La Balanzona (19.4 mg kg^{-1}). In this work, we considered a local geochemical background Sb level at concentrations below 23.4 mg kg^{-1}, which implies clear Sb compositional anomaly in the working area, probably produced by the presence of the Sb mineral masses there. Mining materials indicated extreme Sb concentrations of around 20,000 mg kg^{-1} (Battaglia-Brunet et al., 2021). These values are similar to the highest values published in mining areas (Wang et al., 2010).

The distribution of the main trace elements (Sb, Pb, Cr, Ni) revealed three differentiated zones in the study area: (i) a central zone with high Sb values influenced by the presence of ore deposits and mining work; (ii) a second area located SW and dominated by mafic elements linked with the outcrop of a mass of diabases or dolerites; (iii) a third zone occupied by agricultural soils with Sb values below the local geochemical background or belonging to the transition population data in the mining dispersion area of influence (Fig. 2). The central area extension is controlled by topography due to the location of the ore mass in the highest part of the quartzite relief. Although Sb distribution is favoured by slopes of 11–32%, the area of influence showing concentrations >120 mg kg^{-1} is very narrow, with about 450 m in the direction of the

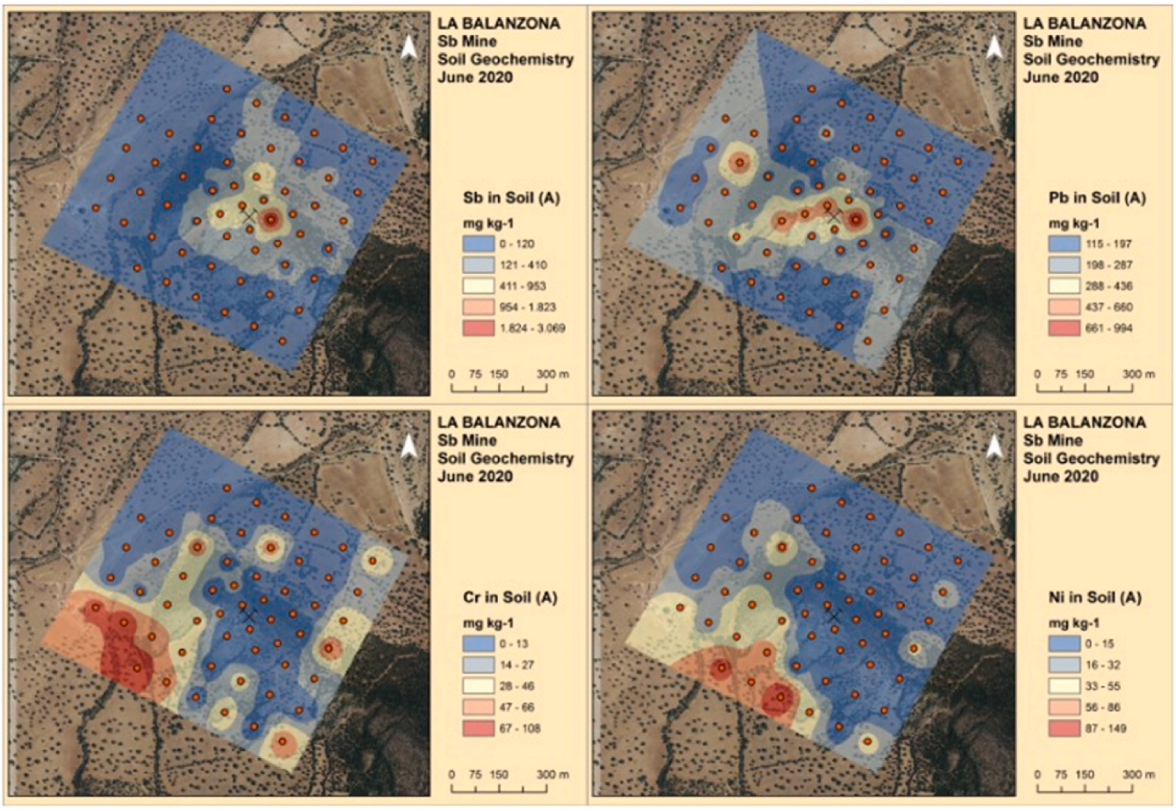

Fig. 2. Dispersion area around the La Balanzona mine of the main monitored trace heavy metals: Sb, Pb, Cr and Ni. Interpolation method: Inverse Distance Weighting. See Fig. 1 for geological features.

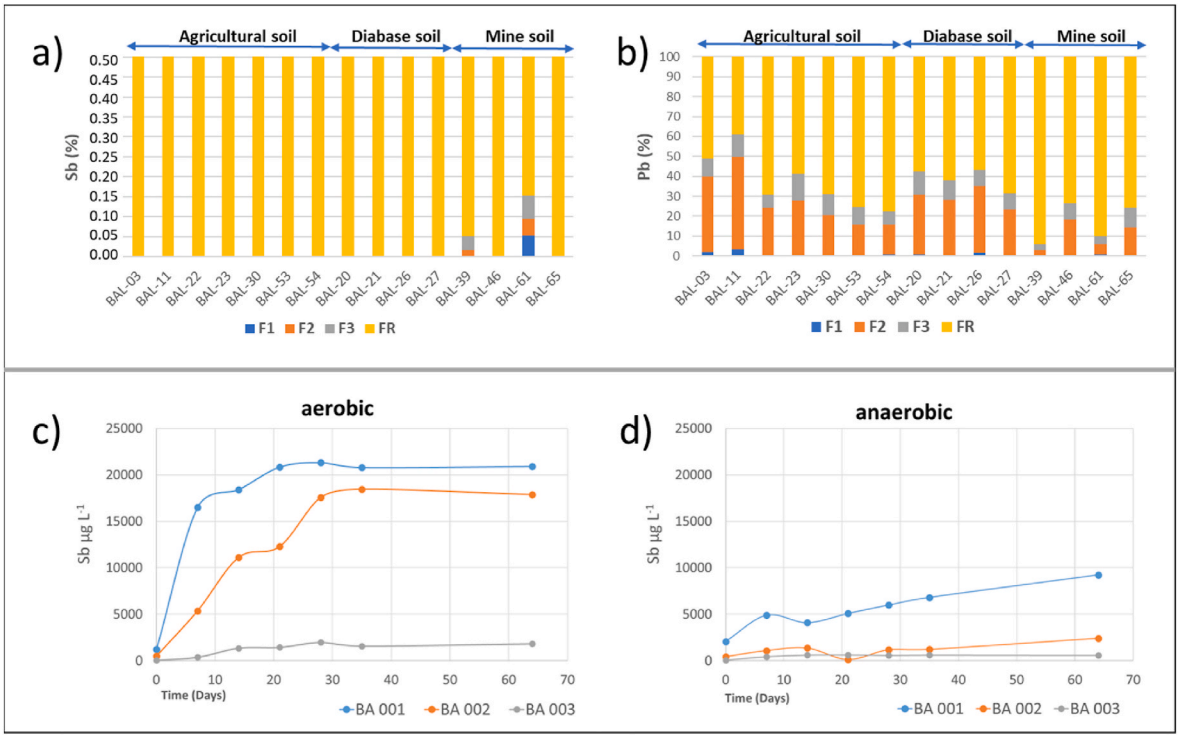

Fig. 3. BCR fractionation for Sb (a) and Pb (b) and long-term soils in leaching tests and evolution of the dissolved Sb concentration in aerobic (c) and anaerobic condition (d).

quartzite strata and 500 m wide in the perpendicular direction towards both sides of the relief. The extension of the areas respectively contaminated by Sb and Pb significantly differs. The Pb contamination area appears to extend more towards the W and SSW directions than the Sb area, perhaps due to differences in Sb–Pb ore deposits emplacement or due to differences in mobility patterns of these two potentially toxic elements. This finding suggests that Pb could be more mobile than Sb.

The second area has a diabase outcrop extension because of the flat topography and without an appreciable slope to favour physical dispersion. The highest Cr and Ni concentrations were 67–108 mg kg^{-1} and 87–149 mg kg^{-1}, respectively, which are much higher than the reference values for Castilla-La Mancha of 56.5 and 20.8 mg kg^{-1}, respectively (Jiménez Ballesta et al., 2010).

The Sb concentration in the third area was below 120 mg kg^{-1} with a coincidental extension of agricultural soils. These soils present anomalous Cl contents, perhaps of anthropic origin, and are mainly from the potash fertilisers extracted from natural deposits (Susarla et al., 1999) and/or the manure originating from intensive livestock activities (Wan et al., 2018).

BCR sequential extraction differentiated four fractions with graded mobility. The first fraction (F1) was rich in species soluble in water, and easily leached by weak acids and associated with soluble carbonates. The second (F2) consisted of easily reducible species associated with Fe and Mn oxyhydroxides. The third fraction (F3) included the easily oxidisable species, mainly associated with organic matter and sulphide minerals. The fourth (F4) contained those species extracted from silicates or sulphides with very low solubility. The BCR extraction data revealed that the residual fraction was the most dominant for Sb, with 99.9% values for all the samples except for two, for which the other fractions reached proportions of 0.15 and 0.05 (Fig. 3a). This means that the amount of Sb in mobile or available fractions was negligible. This is consistent with previous data indicating 97.6–99.6% Sb in residual fractions (Álvarez-Ayuso et al., 2012 and 2022) in agricultural soils polluted by mining activities in the Zamora province (Spain) and in San Antonio mine, respectively. Per land use type, only the very minor Sb fractions F1, F2 and F3 were quantified in mining soils, mainly due to the detection limit of Atomic Absorption analysis (total Sb concentrations in mining soils were much higher than in others). However, Pb behaviour seemed different with a residual fraction that often remained dominant (40–90%), but with large Pb fractions bound to Fe and Mn oxides (F2) and a very low proportion bound to organic matter/sulphides (F3) (Fig. 3b). Some samples showed very small Pb proportions (<5%) easily leached by weak acids and associated with soluble carbonates (F1). Per land use type, the distribution pattern of the Pb fractions seemed more significant, with very constant and large Pb fractions bound to Fe–Mn oxyhydroxides (F3) in diabase soils, and majority residual fractions in mine soils. Agricultural soils presented very wide variability, with similar residual fractions (RF) to those found in diabase soils and a variable Pb proportion bound to Fe–Mn oxyhydroxides.

The long-term leaching tests resulted in greater Sb mobility under aerobic vs. anaerobic conditions (Fig. 3c and d). After 60 leaching days, dissolved Sb represented between 0.1% and 0.3% of the total soil Sb for the anaerobic conditions, and between 0.6% and 1% of the total soil Sb for the aerobic conditions.

3.3. Enzymatic activity (DHA)

Dehydrogenase activity (DHA) was studied in a selection of samples representing different soil types: diabase, agricultural and mining. The results indicated that the DHA values fell within a narrow range (59.4–181.2 μg TPF g^{-1} d^{-1}) and generally took low values. They were much lower than the DHA values described by Campos et al. (2018) for Hg-contaminated soils in Almadenejos (484 ± 269), but similar to those in Hinojosa et al. (2004) for soils contaminated by heavy metals due to the Aznalcollar spill (70 μg TPF g^{-1} d^{-1}) (Fig. S2a), and higher than the DHA values at the San Quintín site, where a Pb–Zn mine obtained 70.98 ± 50.92 for the reference soils near the mine, and 2.85–2.52 in dumps and tailings, respectively (Gallego et al., 2021). A clear gradation of decreasing DHA values was observed for the soils on diabase to agricultural soils and mine soils (the location of these soils is seen in Fig. 2). We think that these DHA differences in the soils on diabase can be explained by compositional differences for being soils under similar physiographical and use conditions as the agricultural soils to the North and South of the quartzite ridge where the stibnite deposit is located. A statistically significant relation was found between SOM and DHA (r^2 = 0.74) (Fig. S2b). It is unclear whether the low DHA values in mine soils were due to low SOM contents because these soils develop in an elevated area with poor edaphic development and sparse forestry, or due to the negative effect of Sb and/or associated elements like Pb on soil microorganisms.

3.4. *Quercus* leaves

In the analysed *Q. rotundifolia* leaves, the identified major elements (>1000 mg kg^{-1}) included Ca, K and Si at average concentrations of 6,722, 4469 and 1363 mg kg^{-1}, respectively. A second group of elements reached significant concentrations: Al (942 mg kg^{-1}), P (741 mg kg^{-1}), Mn (662 mg kg^{-1}), Fe (190 mg kg^{-1}) and Cl (113 mg kg^{-1}). Ti, Zn, Sn, Br, Cu, Sr, Ni, Sb, Rb, Zr and Pb were also identified at trace levels. The Sb concentration range was very narrow (1.45–3.85 mg kg^{-1}) with slight variability. The only elements of the plant bioconcentrates with higher values were Ca, S and Mn and, to a lesser extent, Br. The Sb data population showed an anomaly threshold at 2.51 mg kg^{-1} with a very extensive anomalous data population in the study area (Fig. 4). It can be stated that all the quantified elements had bioaccumulated in leaves by root uptake and translocation to the aerial part or by direct uptake from the atmosphere in the form of gas (especially for Hg, as shown by other studies; see Naharro et al., 2020 and references within).

The Bioaccumulation factors (BAFs) showed very few bioconcentrated elements (BAF >1). On average, only Br, Mn, Ca and S, plus some data about Eu and Cu, presented BAF >1 (Fig. 4). The BAFs of the elements present in mineralisation (Sb and Pb) had very low values in the order of 0.0002–0.1520 for Sb and 0.0000–0.0168 for Pb. These values indicated very poor uptake for both these elements and are similar to those reported for the Bombita mine, a Pb–Zn–Cu mine in Spain (0.006 ± 0.006), but lower than those for other nearby Pb–Zn mines like San Quintín (0.048 ± 0.060) and La Romanilla (0.062 ± 0.071) (Higueras et al., 2017). Antoniadis et al. (2022) described a low absorption capacity of Sb in olive trees. Murciego et al. (2007) shows higher BAF levels for *Dittrichia viscosa* (a shrub plant species) in the San Antonio mine. The distribution of these BAFs in the study area revealed that only Cu bioaccumulated in the central quartzite zone where mineralisation was located, and to a lesser extent Mn, while the other elements had higher BAF values in agricultural soils or on diabase, with Br clearly illustrating this trend (Fig. 4).

3.5. Discussion

Overall, the obtained results describe a barely extended study area (0.6 km^2), in which stibnite (Sb_2S_3) mineralisation is located on the central quartzite massif in a topographically elevated position. Given the elevated physiographic position of the mineralised body, physical and chemical dispersions are favoured, but the dispersion halo of high Sb concentrations does not exceed a radio of 120 m around mining works. The total Sb distribution in the area suggests this element's low mobility. This was confirmed by the BCR extraction carried out for Sb and Pb, which overwhelmingly (>99.9%) indicated Sb proportions in the residual phase, probably linked with sulphides. Pb mobility was greater, with a sum of mobile fractions (F1 + F2 + F3) within the 20–50% range, but no acidity was generated in the area during and after mining exploitation. The effect of Sb and Pb on the enzymatic activity of soil

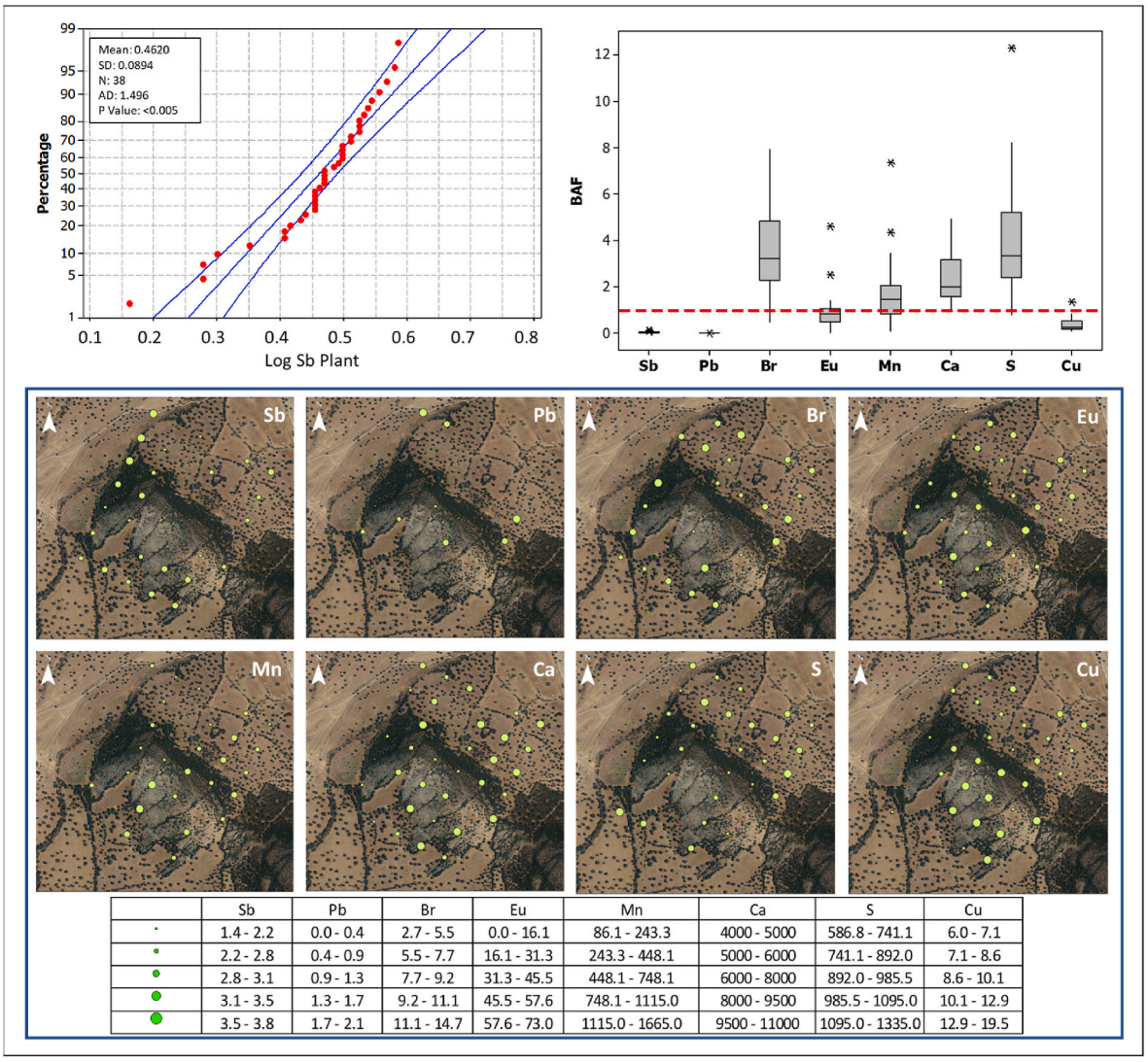

	Sb	Pb	Br	Eu	Mn	Ca	S	Cu
	1.4 - 2.2	0.0 - 0.4	2.7 - 5.5	0.0 - 16.1	86.1 - 243.3	4000 - 5000	586.8 - 741.1	6.0 - 7.1
	2.2 - 2.8	0.4 - 0.9	5.5 - 7.7	16.1 - 31.3	243.3 - 448.1	5000 - 6000	741.1 - 892.0	7.1 - 8.6
	2.8 - 3.1	0.9 - 1.3	7.7 - 9.2	31.3 - 45.5	448.1 - 748.1	6000 - 8000	892.0 - 985.5	8.6 - 10.1
	3.1 - 3.5	1.3 - 1.7	9.2 - 11.1	45.5 - 57.6	748.1 - 1115.0	8000 - 9500	985.5 - 1095.0	10.1 - 12.9
	3.5 - 3.8	1.7 - 2.1	11.1 - 14.7	57.6 - 73.0	1115.0 - 1665.0	9500 - 11000	1095.0 - 1335.0	12.9 - 19.5

Fig. 4. Probability graph of the Sb concentrations in the *Q. rotundifolia* leaves from the La Balanzona mine (left); the bioaccumulation factor for some selected elements (right) and the spatial distribution of the BAFs of some selected elements at the La Balanzona mine (see Fig. 1 for geological features). All values are expressed as mg kg^{-1}.

microorganisms was not significant. Organic matter was a more influential factor on the DHA values than the higher or lower Sb and Pb concentrations in soil. Diquattro et al. (2020) also found very low DHA values in soils doped with Sb (V), and their estimated probable cause was the importance of Sb concentrations in reducing soil enzymatic activity by interacting with the enzyme-substrate complex, enzyme denaturation or interacting with protein-active groups (Nannipieri et al., 2003). In our case, the low SOM values seemed to act as a limiting factor, which could be important given these low DHA values. Finally, the soil-plant transfer was not high for Sb or Pb, although the bioconcentration of other elements (i.e. Mn) was observed in *Q. rotundifolia* leaves.

In this oxidation scenario of a practically monometallic deposit, the BCR sequence extraction results revealed an extremely low proportion of Sb-soluble phases (F1 + F2 + F3) compared to that of Pb. These results suggest an important role of Fe–Mn oxyhydroxides as immobilisers of Pb under oxidising conditions, but not in contrast to Sb as previously described by Belzile et al. (2001). Cappuyns et al. (2021) reported very similar results in mining waste and soils in an Sb mine in Vietnam, where less than 1% of the total Sb content in samples was released to water during short-term leaching tests. Here long-term leaching tests were performed with the La Balanzona soils, whose duration allowed microbial processes to occur, and revealed greater Sb mobility under oxidising conditions vs. reducing conditions. These results agree with previous reports (Casiot et al., 2007; Li et al., 2022), which suggest that microbial sulphur and Sb (III) oxidising activities might mobilise Sb. However, this mobilisation implies a long contact time between solids and water, which is hardly a compatible scenario to the climate and topographic conditions at the La Balanzona site. In another context, Okkenhaug et al. (2011) described high Sb leaching levels at an active mining site in China controlled by the presence of Ca $[Sb(OH)_6]_2$. However, this case is not comparable to the La Balanzona mine conditions.

The herein described low Sb mobility in an oxidising environment, together with no relation linking Sb, Pb and soil enzymatic activity, constitute a framework of favourable conditions for exploiting similar deposits under comparable environmental conditions without having to implement expensive mining effluent control systems that limit the dispersion of the extracted element. However, the use of soil geochemical data to prospect Sb deposits is seriously limited by this low mobility. Nevertheless, by using pathfinder elements (As, Mn) patterns, in which single-element Sb patterns failed, could be a way to improve the detection of Sb mineralisation (Lemière et al., 2020). The dispersion of the elements of an ore deposit depends on factors like redox, acid-base or

hydrolysis processes that recycle minerals and their associated elements by incorporating them into soil. There are three components in the secondary geochemical dispersion of elements: physical, chemical or biogenic. In the Balanzona mine, only physical dispersion seems to act because mineralisation is located in a topographically elevated position on rocks that withstand weathering and generate a mountainous relief. Chemical dispersion seems very limited by the low solubility of Sb compounds, a predictable fact for primary minerals, but not for oxidised phases. It is necessary to highlight that oxidised phases in quartzite are scarce and restricted to the rock fractures in the most external zones of quartzites.

What do we know about biogenic dispersion? The Sb contents in *Q. rotundifolia* leaves do not offer promising results, with very narrow variability and their spatial distribution is incoherent with the presence of mineralisation. In general terms, woody vegetation often accumulates more Sb than non-woody vegetation. Species like *Picea glauca* are capable of bioaccumulating Sb in their roots (Busby et al., 2021), although it seems that translocation to the aerial part is inhibited, probably due to the element's toxic character. Guarino et al. (2021) described high Sb levels in *Olea europaea* leaves whose origin is airborne particles. So woody tree leaves are not expected to be used for prospecting Sb ore deposits by remote sensing technologies (Wang et al., 2018), but can provide valuable data as biomonitors during mining operations.

4. Conclusions

Sb mobility and transfer were investigated in an abandoned mine with a semi-arid climate where oxidation processes predominate. The main findings are:

- Very high total Sb contents appear in mining materials (max: 8450 mg kg^{-1}), dispersed in a very small area around the ore deposit (<300 m). Pb contents are also significant and form part of the oxidised Sb phases
- BCR extraction indicates extremely low Sb mobility, supported by a slight Sb transfer to the leaves of the most conspicuous plant species in the area: *Quercus rotundifolia* trees
- The effect of Sb on soil enzymatic activity could not be established because soils showed slight enzymatic activities related to poorly developed soils with low organic matter content

The La Balanzona mine results limit Sb chemical dispersion under a semi-arid climate and with absence of acid mine drainage generation. This context restricts the geochemical exploration possibilities of Sb ore deposits but favours their mining exploitation by limiting effluent control measures.

Consent to publish

José María Esbrí, Researcher, PhD, as responsible of the manuscript entitled "Evaluation of antimony availability in a mining context: impact for the environment, and for mineral exploration and exploitation", authored by myself and Carmelo M. Minang, graduate; Sofía Rivera, MsC; Mercedes Madrid-Illescas, MsC; Eva García-Noguero, PhD; Ana Gonzalez-Valois, MsC; Maite Maguregui, PhD; Hugues Thouin, PhD; Fabienne Battaglia-Brunet; PhD; Eric Gloaguen, PhD and Pablo León Higueras, PhD. On behalf of the rest of coauthors, with this document I warrantee and sign that this manuscript does not contains any individual person's data in any form (including any individual details, images or videos).

-Authors contributions

José María Esbrí (JME), Researcher, PhD, as responsible of the manuscript entitled "Evaluation of antimony availability in a mining context: impact for the environment, and for mineral exploration and exploitation", authored by myself and Carmelo M. Minang (CM), graduate; Sofía Rivera, MsC; Mercedes Madrid-Illescas (MMI), MsC; Eva García-Noguero (EG), PhD; Ana Gonzalez-Valois (AG), MsC; Maite Maguregui (MM), PhD; Hugues Thouin (HT), PhD; Fabienne Battaglia-Brunet (FB); PhD; Eric Gloaguen (EG), PhD and Pablo León Higueras (PH), PhD. On behalf of the rest of coauthors, with this document I warrantee and sign that the contributions done by the listed authors have been the following:

- Conceptualization JME, FBB, MM, EG, PH,
- Data curation JME, FB, HT, PH
- Formal analysis JME, HT
- Funding acquisition EG and PH
- Investigation JME, CM, SR, HT, FB, PH
- Methodology JME, CM, SR, MMI, EG, AG, HT, FB
- Project administration EG and PH
- Resources JME
- Software JME, SR, HT, - Supervision JME, EG, FB, MM, PH,
- Validation JME, HT, PH
- Visualization JME, PH
- Roles/Writing – original draft JME, MM, FB, PH
- Writing – review & editing JME, MM, FB, EG, PH

Funding information

This study is a contribution to the AUREOLE Project, funded by the ERA-MIN2 European Project through the Spanish PCI2019-103779 and French ANR-19-MIN2-0002-01 grant agreements.

Declaration of competing interest

The authors declare that they have no known competing financial interests or personal relationships that could have appeared to influence the work reported in this paper.

Data availability

Data will be made available on request.

Acknowledgements

We wish to thank Helen Warburton for proofreading the manuscript, and also the IRICA-UCLM laboratories for their analytical support in the mineralogical determinations.

Appendix A. Supplementary data

Supplementary data to this article can be found online at https://doi.org/10.1016/j.chemosphere.2022.137086.

References

Álvarez-Ayuso, E., Otones, V., Murciego, A., García-Sánchez, A., Regina, I.S., 2012. Antimony, arsenic and lead distribution in soils and plants of an agricultural area impacted by former mining activities. Sci. Total Environ. 439, 35–43. https://doi.org/10.1016/j.scitotenv.2012.09.023.

Álvarez-Ayuso, E., Murciego, A., Rodríguez, M.A., Fernández-Pozo, L., Cabezas, J., Naranjo-Gómez, J.M., Mosser-Ruck, R., 2022. Antimony distribution and mobility in different types of waste derived from the exploitation of stibnite ore deposits. Sci. Total Environ. 816. https://doi.org/10.1016/j.scitotenv.2021.151566.

Antoniadis, V., Thalassinos, G., Levizou, E., Wang, J., Wang, S.-., Shaheen, S.M., Rinklebe, J., 2022. Hazardous enrichment of toxic elements in soils and olives in the urban zone of lavrio, Greece, a legacy, millennia-old silver/lead mining area and related health risk assessment. J. Hazard Mater. 434 https://doi.org/10.1016/j.jhazmat.2022.128906.

Arribas, A., Gumiel, P., 1984. First occurrence of a strata-bound Sb-W-Hg deposit in the Spanish hercynian massif. In: Wauschkuhn, A., Kluth, C., Zimmermann, R.A. (Eds.), Syngenesis and Epigenesis in the Formation of Mineral Deposits. Springer, Berlin, Heidelberg, pp. 468–481. https://doi.org/10.1007/978-3-642-70074-3_43.

Ashley, P.M., Craw, D., Graham, B.P., Chappell, D.A., 2003. Environmental mobility of antimony around mesothermal stibnite deposits, new south Wales, Australia and southern New Zealand. J. Geochem. Explor. 77 (1), 1–14. https://doi.org/10.1016/S0375-6742(02)00251-0.

Barajas, M., 2008. Ensayos de metabolismo microbiano en suelo: actividad deshidrogenasa y tasa de mineralizacion del nitrogeno. In: Ramírez, P., Mendoza, A. (Eds.), Ensayos toxicologicos para la evaluacion de sustancias químicas en agua y suelo: la experiencia en Mexico. Inst. Nac. de Ecol, Mexico.

Battaglia-Brunet, F., Thouin, H., Esbri, J.M., Garcia-Noguero, E.M., Lorenzo, S., Higueras, P., Gloaguen, E., 2021. Mobility of Antimony in Samples from Diverse Environmental Compartments of Sb Mines in Spain: Leaching Experiments in Oxidizing and Reducing Conditions abstract EGU21-2781. Available at: https://meetingorganizer.copernicus.org/EGU21/EGU21-2781.html. (Accessed 1 April 2022). accessed.

Belzile, N., Chen, Y., Wang, Z., 2001. Oxidation of antimony (III) by amorphous iron and manganese oxyhydroxides. Chem. Geol. 174, 379–387. https://doi.org/10.1016/S0009-2541(00)00287-4.

Boixereu Vila, E., Fernández-Leyva, C., 2019. An early exploitation of the antimony in santa cruz de Mudela (ciudad real) during the modern age (1576-1803), 2019 De. Re Met. 32, 87–94. http://www.sedpgym.es/publicaciones/revista-de-re-metallica/indices-resumenes-y-textos-completos-de-re-metallica/17-publicaciones/de-re-metallica/186-de-re-metallica-n-32-enero-junio-2019. (Accessed 2 November 2022).

Bolan, N., Kumar, M., Singh, E., Kumar, A., Singh, L., Kumar, S., Siddique, K.H.M., 2022. Antimony contamination and its risk management in complex environmental settings: a review. Environ. Int. 158 https://doi.org/10.1016/j.envint.2021.106908.

Borčinová Radková, A., Jamieson, H.E., Campbell, K.M., 2020. Antimony mobility during the early stages of stibnite weathering in tailings at the beaver brook sb deposit, newfoundland. J. Appl. Geochem. 115 https://doi.org/10.1016/j.apgeochem.2020.104528.

Busby, R.R., Barbato, R.A., Jung, C.M., Bednar, A.J., Douglas, T.A., Ringelberg, D.B., Indest, K.J., 2021. Alaskan plants and their assembled rhizosphere communities vary in their responses to soil antimony. Appl. Soil Ecol. 167 https://doi.org/10.1016/j.apsoil.2021.104031.

Campos, J.A., Esbrí, J.M., Madrid, M.M., Naharro, R., Peco, J., García-Noguero, E.M., Amorós, J.A., Moreno, M.M., Higueras, P., 2018. Does mercury presence in soils promote their microbial activity? the Almadenejos case (Almaden mercury mining district, Spain). Chemosphere 201, 799–806. https://doi.org/10.1016/j.chemosphere.2018.02.163.

Cappuyns, V., Van Campen, A., Helser, J., 2021. Antimony leaching from soils and mine waste from the mau due antimony mine, north-Vietnam. J. Geochem. Explor. 220. https://doi.org/10.1016/j.gexplo.2020.106663.

Casida, L.E., 1977. Microbial metabolic activity in soil as measured by dehydrogenase determinations. Appl. Environ. Microbiol. 34, 630–636. https://doi.org/10.1128/aem.34.6.630-636.1977.

Casiot, C., Ujevic, M., Munoz, M., Seidel, J.L., Elbaz-Poulichet, F., 2007. Antimony and arsenic mobility in a creek draining an antimony mine abandoned 85 years ago (upper orb basin, France). J. Appl. Geochem. 22 (4), 788–798. https://doi.org/10.1016/j.apgeochem.2006.11.007.

European Commision, 2020. Study on the EU's List of Critical Raw Materials (2020). Critical Raw Materials Factsheets (Final), 2020. Publications Office of the European Union, Luxembourg. Available at: https://rmis.jrc.ec.europa.eu/uploads/CRM_2020_Factsheets_critical_Final.pdf. (Accessed 2 February 2022). accessed.

Courtin-Nomade, A., Rakotoarisoa, O., Bril, H., Grybos, M., Forestier, L., Foucher, F., Kunz, M., 2012. Weathering of Sb-rich mining and smelting residues: insight in solid speciation and soil bacteria toxicity Chem. Erde-Geochem. 72, 29–39. https://doi.org/10.1016/j.chemer.2012.02.004.

Delgado, J., Barba-Brioso, C., Nieto, J.M., Boski, T., 2011. Speciation and ecological risk of toxic elements in estuarine sediments affected by multiple anthropogenic contributions (Guadiana saltmarshes, SW Iberian peninsula): I. surficial sediments. Sci. Total Environ. 409 (19), 3666–3679. https://doi.org/10.1016/j.scitotenv.2011.06.013.

Diquattro, S., Garau, G., Mangia, N.P., Drigo, B., Lombi, E., Vasileiadis, S., Castaldi, P., 2020. Mobility and potential bioavailability of antimony in contaminated soils: short-term impact on microbial community and soil biochemical functioning. Ecotoxicol. Environ. Saf. 196 https://doi.org/10.1016/j.ecoenv.2020.110576.

ERAMIN, 2021. Raw materials for the sustainable development and the circular economy. Available at: https://www.era-min.eu/. Accessed 02 November 2021.

Esbrí, J.M., Rivera, S., Tejero, J., Higueras, P.L., 2021. Feasibility study of fluorescent lamp waste recycling by thermal desorption. Environ. Sci. Pollut. Res. 28 (43), 61860–61868. https://doi.org/10.1007/s11356-021-16800-3.

Filella, M., Belzile, N., Lett, M., 2007. Antimony in the environment: a review focused on natural waters. III. microbiota relevant interactions. Earth Sci. Rev. 80 (3–4), 195–217. https://doi.org/10.1016/j.earscirev.2006.09.003.

Gallego, S., Esbrí, J.M., Campos, J.A., Peco, J.D., Martin-Laurent, F., Higueras, P., 2021. Microbial diversity and activity assessment in a 100-year-old lead mine. J. Hazard Mater. 410 https://doi.org/10.1016/j.jhazmat.2020.124618.

Gonzalez-Valoys, A.C., Esbrí, J.M., Campos, J.A., Arrocha, J., García-Noguero, E.M., Monteza-Destro, T., Martínez, E., Jiménez-Ballesta, R., Gutiérrez, E., Vargas-Lombardo, M., Garcia-Ordiales, E., García-Giménez, R., García-Navarro, F.J., Higueras, P., 2021. Ecological and health risk assessments of an abandoned gold mine (Remance, Panama): complex scenarios need a combination of indices. Int. J. Environ. Res. Publ. Health 18, 9369. https://doi.org/10.3390/ijerph18179369.

Guarino, F., Improta, G., Triassi, M., Castiglione, S., Cicatelli, A., 2021. Air quality biomonitoring through olea europaea L.: the study case of "Land of pyres". Chemosphere 282. https://doi.org/10.1016/j.chemosphere.2021.131052.

Gumiel, P., Arribas, A., 1987. Antimony deposits in the Iberian peninsula. Econ. Geol. 82 (6), 1453–1463. https://doi.org/10.2113/gsecongeo.82.6.1453.

Higueras, P., Esbrí, J., García-Ordiales, E., González-Corrochano, B., López-Berdonces, M., García-Noguero, E., Alonso-Azcárate, J., Martínez-Coronado, A., 2017. Potentially harmful elements in soils and holm-oak trees (Quercus ilex L.) growing in mining sites at the Valle de Alcudia Pb-Zn district (Spain)– Some clues on plant metal uptake, 2017 J. Geochem. Explor. 182, 166–179. https://doi.org/10.1016/j.gexplo.2016.07.017.

Hinojosa, M.B., Carreira, J.A., García-Ruíz, R., Dick, R.P., 2004. Soil moisture pretreatment effects on enzyme activities as indicators of heavy metal-contaminated and reclaimed soils. Soil Biol. Biochem. 36, 1559–1568. https://doi.org/10.1016/j.soilbio.2004.07.003.

Jiménez Ballesta, R., Conde Bueno, P., Martín Rubí, J.A., García Giménez, R., 2010. Geochemical background levels and influence of the geological setting on pedogeochemical baseline concentrations of trace elements in selected soils of Castilla-la Mancha (Spain). [Niveles de fondo geoquímico e influencia del marco geológico en las concentraciones edafogeoquímicas de base de suelos seleccionados de Castilla-La Mancha] Estudios Geologicos 66 (1), 123–130. https://doi.org/10.3989/egeol.40214.119.

Johnston, S.G., Bennet, W.W., Dorian, N., Hockmann, K., Karimian, N., Burton, E.D., 2020. Antimony and arsenic speciation, redox-cycling and contrasting mobility in a mining-impacted river system. Sci. Total Environ. 710, 136354 https://doi.org/10.1016/j.scitotenv.2019.136354.

Lemière, B., Melleton, J., Auger, P., Derycke, V., Gloaguen, E., Bouat, L., Mikšová, D., Filzmoser, P., Middleton, M., 2020. pXRF measurements on soil samples for the exploration of an antimony deposit: example from the vendean antimony district (France). Minerals 10, 724. https://doi.org/10.3390/min10080724.

Li, Y., Hu, X., Ren, B., 2016. Treatment of antimony mine drainage: challenges and opportunities with special emphasis on mineral adsorption and sulfate reducing bacteria. Water Sci. Technol. 73 (9), 2039–2051. https://doi.org/10.2166/wst.2016.044.

Li, X., Chaoyang, L., Deng, L., Liyuan, M., Xuan, Q., Hongmei, W., Xiaolu, L., 2022. Antimony transformation and mobilization from stibnite by an antimonite oxidizing bacterium Bosea sp. AS-1. J. Environ. Sci. 111, 273–281. https://doi.org/10.1016/j.jes.2021.03.042.

Loni, P.C., Wu, M., Wang, W., Wang, H., Ma, L., Liu, C., Song, Y., H.T, O., 2020. Mechanism of microbial dissolution and oxidation of antimony in stibnite under ambient conditions. J. Hazard Mater. 385, 121561 https://doi.org/10.1016/j.jhazmat.2019.121561.

Melaku, S., Dams, R., Moens, L., 2005. Determination of trace elements in agricultural soil samples by inductively coupled plasma-mass spectrometry: microwave acid digestion versus aqua regia extraction. Anal. Chim. Acta 543, 117–123. https://doi.org/10.1016/j.aca.2005.04.055.

Montejo, M., Torres, C.P., Martínez, A., Tenorio, J.A., Cruz, M.R., Ramos, F.R., Cuevas, M.C., 2012. Técnicas para el análisis de actividad enzimática en suelos. In: Cuevas, M.C., Espinosa, G., Ilizaliturri, C., Mendoza, A. (Eds.), Métodos ecotoxicológicos para la evaluación de suelos contaminados con hidrocarburos, INECC, México.

Moore, M., Reynolds, R.C., 1997. X-Ray Diffraction and the Identification and Analysis of Clay Minerals, second ed. Oxford University Press, England.

Murciego, A.M., Sánchez, A.G., González, M.A.R., Gil, E.P., Gordillo, C.T., Fernández, J. C., Triguero, T.B., 2007. Antimony distribution and mobility in topsoils and plants (*Cytisus striatus, Cistus ladanifer* and *Dittrichia viscosa*) from polluted Sb-mining areas in Extremadura (Spain). Environ. Pollut. 145, 15–21. https://doi.org/10.1016/j.envpol.2006.04.004.

Naharro, R., Esbrí, J.M., Amorós, J.A., Higueras, P.L., 2020. Experimental assessment of the daily exchange of atmospheric mercury in epipremnum aureum. Environ. Geochem. Health 42 (10), 3185–3198. https://doi.org/10.1007/s10653-020-00557-8.

Nannipieri, P., Ascher, J., Ceccherini, M., Landi, L., Pietramellara, G., Renella, G., 2003. Microbial diversity and soil functions. Eur. J. Soil Sci. 54 (4), 655–670. https://doi.org/10.1046/j.1351-0754.2003.0556.x.

Okkenhaug, G., Zhu, Y.G., Luo, L., Lei, M., Li, X., Mulder, J., 2011. Distribution, speciation and availability of antimony (Sb) in soils and terrestrial plants from an active Sb mining area, 2011 Environ. Pollut. 159, 2427–2434. https://doi.org/10.1016/j.envpol.2011.06.028.

Ortega, L., Oyarzun, R., Gallego, M., 1996. The Mari Rosa late Hercynian Sb-Au deposit, western Spain. Miner. Deposita 31, 172–187. https://doi.org/10.1007/BF00204025.

Quevauviller, P., Rauret, G., López-Sánchez, J., Rubio, R., Ure, A., Muntau, H., 1997. Certification of trace metal extractable contents in a sediment reference material (CRM 601) following a three-step sequential extraction procedure. Sci. Total Environ. 205 (2–3), 223–234. https://doi.org/10.1016/S0048-9697(97)00205-2.

Rivera-Jurado, S., Lorenzo, S., Monsuy, C., Esbrí, J., Gloaguen, E., Higueras, P., 2021. Regional Soil Geochemistry for Sb and Hg in Guadalmez and Almadén Synclines, South-Central Spain session ERE5.6/GMPV5.4, abstract EGU21-4850. Available at: https://meetingorganizer.copernicus.org/EGU21/EGU21-4850.html. (Accessed 1 April 2022). Accessed.

Roper, A.J., Williams, P.A., Filella, M., 2012. Secondary antimony minerals: phases that control the dispersion of antimony in the supergene zone. Chem. Erde 72 (4), 9–14. https://doi.org/10.1016/j.chemer.2012.01.005.

Sahuquillo, A., López-Sánchez, J.F., Rubio, R., Rauret, G., Thomas, R.P., Davidson, C.M., Ure, A.M., 1999. Use of a certified reference material for extractable trace metals to assess sources of uncertainty in the BCR three-stage sequential extraction procedure. Anal. Chim. Acta 382 (3), 317–327. https://doi.org/10.1016/S0003-2670(98)00754-5.

Schwarz-Schampera, U., 2014. Antimony. In: Gunn, Gus (Ed.), Critical Metals Handbook. American Geophysical Union - John Wiley & Sons, Ltd., pp. 70–98

Steely, S., Amarasiriwardena, D., Xing, B., 2007. An investigation of inorganic antimony species and antimony associated with soil humic acid molar mass fractions in contaminated soils. Environ. Pol. 148, 590–598. https://doi.org/10.1016/j.envpol.2006.11.031.

Susarla, S., Collette, T.W., Garrison, A.W., Wolfe, N.L., Mccutcheon, S.C., 1999. Perchlorate identification in fertilizers. Environ. Sci. Technol. 33 (19), 3469–3472. https://doi.org/10.1021/es990577k.

Szakall, S., Papp, G., Sajo, I., Kovacs, A., 2000. Antimony oxide minerals from Hungary. Acta Minerol.-Petrogr. (Szeged) 61, 31–62.

European Union, 2020. Critical Raw materials resilience: charting a path towards greater security and sustainability. Available at: https://eur-lex.europa.eu/legal-content/EN/TXT/?uri=CELEX:52020DC0474. (Accessed 2 November 2021). Accessed.

USEPA, 2007. Method 3051a microwave assisted acid digestion of sediments, sludges, soils, and oils, 2007 ReVision 1, 30. Available at: https://www.epa.gov/sites/default/files/2015-12/documents/3051a.pdf. (Accessed 26 April 2022).

Verbeeck, M., Thiry, Y., Smolders, E., 2020. Soil organic matter affects arsenic and antimony sorption in anaerobic soils. Environ. Pollut. 257, 113566 https://doi.org/10.1016/j.envpol.2019.113566.

Wan, D., Wu, L., Liu, Y., Zhao, H., Fu, J., Xiao, S., 2018. Adsorption of low concentration perchlorate from aqueous solution onto modified cow dung biochar: effective utilization of cow dung, an agricultural waste. Sci. Total Environ. 636, 1396–1407. https://doi.org/10.1016/j.scitotenv.2018.04.431.

Wang, X., He, M., Xie, J., Xi, J., Lu, X., 2010. Heavy metal pollution of the world largest antimony mine-affected agricultural soils in Hunan province (China). J. Soils Sediments 10, 827–837. https://doi.org/10.1007/s11368-010-0196-4.

Wang, F., Gao, J., Zha, Y., 2018. Hyperspectral sensing of heavy metals in soil and vegetation: feasibility and challenges. SPRS J. Photogramm. Remote Sens. 136, 73–84. https://doi.org/10.1016/j.isprsjprs.2017.12.003.